Journal of King Saud University – Engineering Sciences (2013) xxx, xxx–xxx

King Saud University

Journal of King Saud University – Engineering Sciences

www.ksu.edu.sa
www.sciencedirect.com

ORIGINAL ARTICLES

Experimental and theoretical investigations of scour at bridge abutment

Y.Abdallah Mohamed [a,*,1], G.Mohamed Abdel-Aal [b], T.Hemdan Nasr-Allah [c], Awad A. Shawky [d]

[a] Associate Professor, Zagazig University, Faculty of Engineering, Egypt
[b] Professor of hydrauluics, Zagazig University, Faculty of Engineering, Egypt
[c] Assistant Professor, Benha University, Faculty of Engineering, Egypt
[d] Demonstrator, Benha University, Faculty of Engineering, Egypt

Received 17 February 2013; accepted 26 September 2013

KEYWORDS

Numerical models;
Bridge abutments;
Local scour;
SSIIM

Abstract Numerical and experimental studies were carried out to investigate the effect of different contraction ratios and entrance angles of bridge abutment on local scour depth. A 3-D numerical model is developed to simulate the scour at bridge abutment. This model solves 3-D Navier–Stokes equations and a bed load conservation equation. The $k-\varepsilon$ turbulence model is used to solve the Reynolds-stress term. In addition, the model verification is made by comparing the computed results with existing experimental data. The results show the ability of the numerical model to simulate local scouring at bridge abutments for different contraction ratios and entrance angles of abutment with high accuracy. The determination coefficient and mean relative absolute error, in average, are 0.95 and, 0.12, respectively.

1. Introduction

The scour is a result of the erosive action of flowing water, excavating and carrying away material from the bed and banks of streams and from around the piers and abutments of bridges (Richardson and Davis, 2001). Such scour around pier and pile supported structures and abutments can result in structural collapse and loss of life and property. Richardson and Abed (1993), quoted in a study produced in 1973 for the U.S. Federal Highway Administration that concluded of 383 bridge failures, 25% involved pier damage and 72% involved abutment damage. The total scour at a river crossing consists of three components: general scour, contraction scour, and local scour (Cheremisinoff et al., 1987). Local scour occurs around piers, abutments, spurs and embankments, which is caused by the acceleration of the flow and the development of vortex systems induced by these obstructions to the flow. Many studies have been carried out to develop the relationships for predicting the maximum scour depth at bridge piers under clear-water scour condition and these relations have been used

* Corresponding author. Address: College of Engineering, Jazan University, Saudi Arabia. Tel.: +966 551195776.
E-mail addresses: ymoussa@jazanu.edu.sa, yasser_eng1997@zu.edu.eg (Y. Mohamed).
[1] Sabbatical Leave from Water Engineering Department, Zagazig University.

Peer review under responsibility of King Saud University.

ELSEVIER Production and hosting by Elsevier

1018-3639 © 2013 Production and hosting by Elsevier B.V. on behalf of King Saud University.
http://dx.doi.org/10.1016/j.jksues.2013.09.005

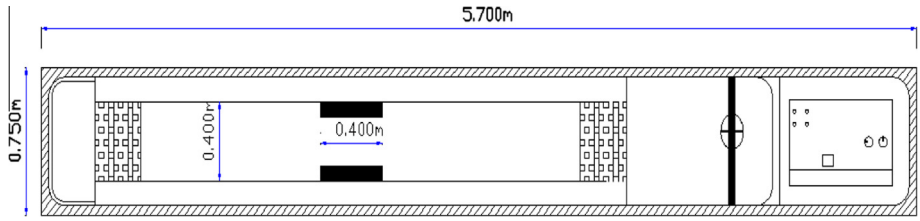

Figure 1 Definition sketch of a re-circulating flume.

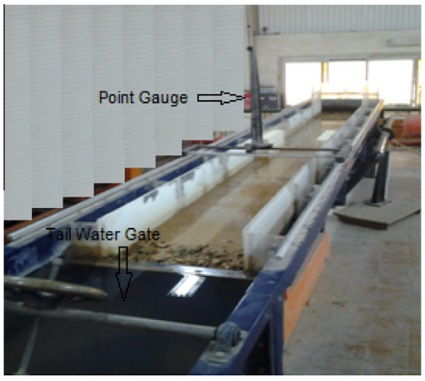

Photo 1 Re-circulating flume.

Photo 2 Different shapes of abutment.

extensively for designing purposes (Dehghani et al., 2009). Lots of researches are carried out to minified the scour dimensions by implementing a circular collar around the pier (Zarrati et al., 2004, 2006; Alabi, 2006; Moncada-M et al., 2009; Abdel-Aal and Mohamed, 2010; Abdel-Aal et al., 2008), submerged vanes (Odgaard and Wang, 1987), a slot through the pier (Chiew, 1992; Grilmaldi et al., 2009; Gaudio et al., 2012, Tafarojnoruz et al., 2010, 2012). The guide wall was used to protect the scour depth at bridge abutment (Fathi et al., 2011). Effect of weed accumulation on scour depth around bridge piers was investigated by Mowafy and EI-Saed (2000). The effect of constructing two adjacent bridges on the flow characteristics and local scour around bridge piers was discussed by Mowafy and Fahmy (2001). Melville (1992) and Melville (1997) presented an integrating approach to the estimation of local scour depth at bridge piers and abutments. Scour around bridge abutment is studied experimentally by-Hua (2005), Abou-Seida et al. (2009) and Kose and Yanmaz (2010). Gene expression programming and artificial neural networks were used to predict the time variation of scour depth at a short abutment by Mohammadpour et al. (2013). The scour computation is considered as a complicated process and time consuming, so, many soft-wares were created and applied to compute scour around bridge piers. Several numerical models have been constructed for simulating the 3D flow field and bed

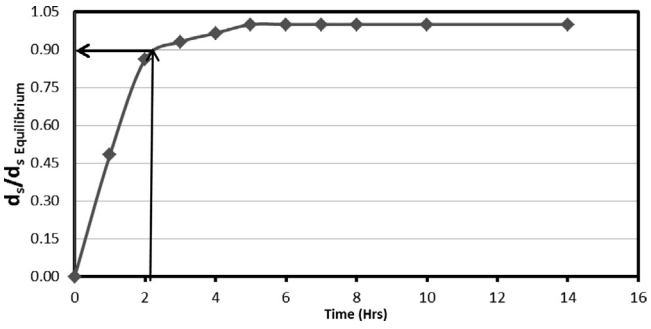

Figure 2 Ratio of maximum to equilibrium scour depths ($d_s/d_{s\ \text{Equilibrium}}$) versus time.

variations around bridge piers. Scour around bridge piers was numerically simulated by Olsen and Melaaen (1993), Dou (1997), Richardson and Panchang (1998)and Tseng et al. (2000). In addition, numerical models are also presented to simulate the scour depth around bridge abutment by Morales and Ettema (2011) and Taymaz et al. (2011). In this study, the local scour around bridge abutment was studied experimentally and numerically. The effects of different contraction

Table 1 Details of experimental conditions.

Discharge (L/s)	3.5	Median sand size (mm)	1.77
Abutment width (b) cm	3.75, 5.0, and 7.5	Flow depth (cm)	3–7
Abutment entrance angle	90°, 60°, 45°, 30°, 15°, and 10°	Froude Number	0.20–0.55

Please cite this article in press as: Mohamed, Y.A. et al., Experimental and theoretical investigations of scour at bridge abutment. Journal of King Saud University – Engineering Sciences (2013), http://dx.doi.org/10.1016/j.jksues.2013.09.005

ratios of bridge and entrance angles at the upstream of bridge abutment, on local scour depth are investigated. The numerical models were created by using SSIIM (sediment simulation in water intake with multiblock option) program. This 3D CFD model was based on the finite volume method to solve the Navier–Stokes equations, Olsen 2007.

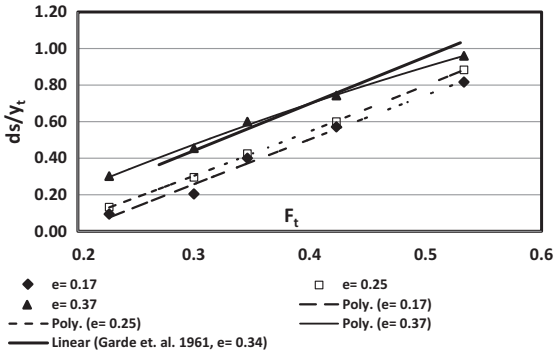

Figure 3 The relationship between the F_t and d_s/y_t for different contraction ratios.

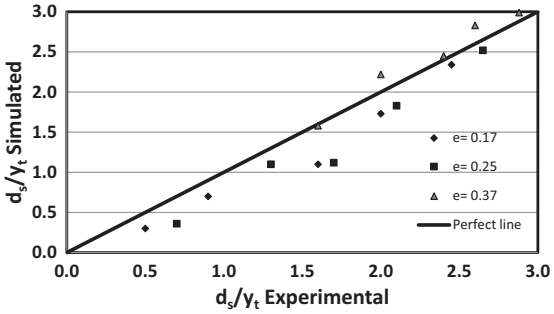

Figure 5 Simulated versus experimental values for d_s/y_t at $Q = 3.5$ L/s, and different contraction ratios (e).

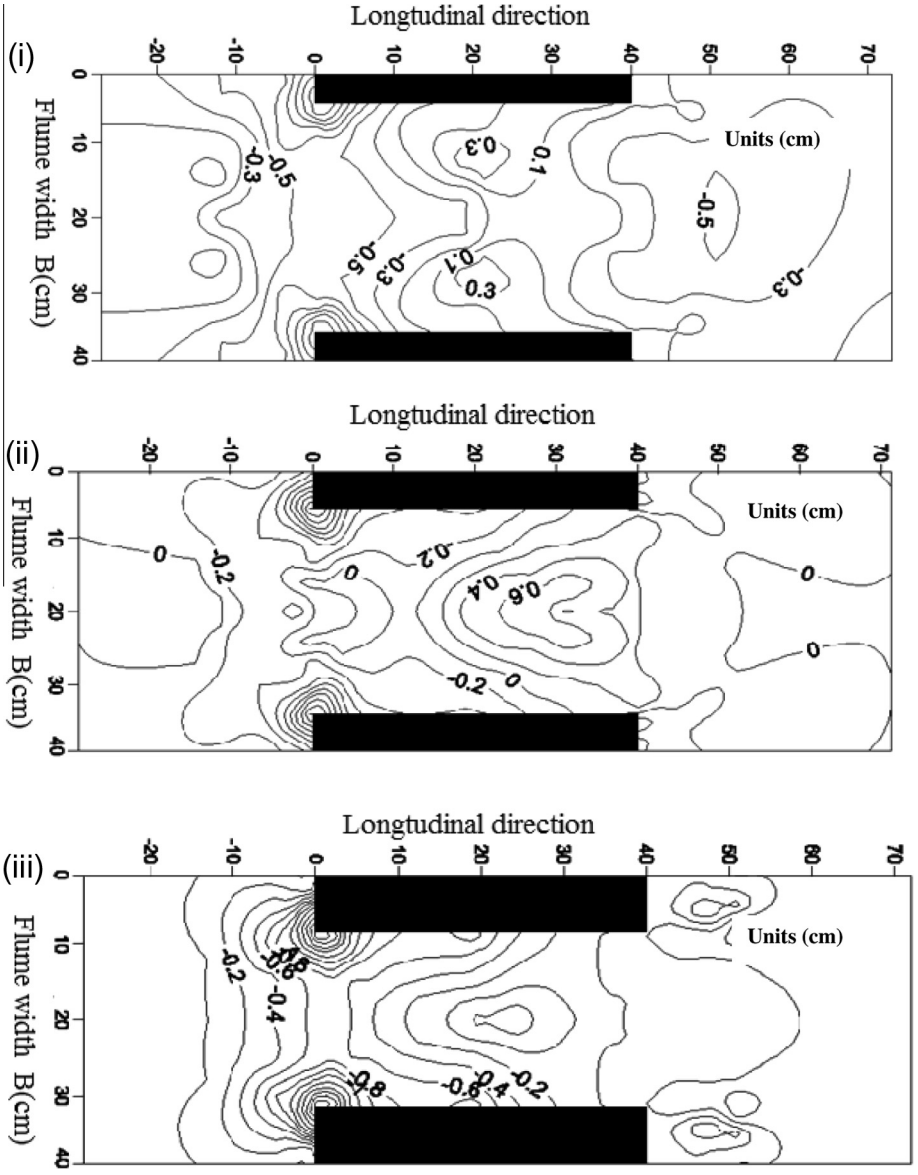

Figure 4 Scour contour maps for (i) $e = 0.17$, (ii) $e = 0.25$, and (iii) $e = 0.37$ at $F_t = 0.35$.

2. Experimental work

The experimental work was carried out in a re-circulating channel with 4 m length, 20 cm depth and 40 cm width, (Fig. 1, and Photo 1). Stones of different sizes were used at the entrance to damp carefully disturbances. The discharge was measured using a pre-calibrated orifice meter. The median sand size (D50) is 1.77 mm. The sediment is to be considered as uniform at which the geometric stander deviation of the particle size distribution is less than 1.3, ($\sigma_g = D_{84}/D_{50} = 1.29$). The experimental work was conducted under the clear-water condition. Clear water scour occurs for velocities up to the threshold for the general bed movement, i.e., $U/U_c \leqslant 1$ (U, is the approach flow velocity, and U_c, is mean approach velocity at the threshold condition) (Melville, 1997). In the present study the value of U/U_c equals 0.7, (i.e., clear water scour). For each test of the experimental program, the sand was leveled along the entire length of flume using a wooden screed with the same width as the flume. The sand level was checked at random points with a point gauge. The flume was slowly filled with water upto the required depth. The pump was then turned on and its speed increased slowly until the desired flow rate was achieved, after that the tailgate was adjusted to get the required water depth. At the end of the test the pump was turned off and the flume was drained slowly without disturbing the scour topography. The bed topography was measured with point gauge with 0.01 mm accuracy on a grid with meshes of 3 cm × 3 cm (sometimes 1 cm × 1 cm depending on the bed topography) over an area of 2.5 m × 0.4 m spanning between 1.0 m upstream and 1.1 m downstream from the abutment. The grid pattern was dense to obtain accurate bed topography at the end of each experiment. Wooden abutments with 40 cm length and different widths were installed in the channel sides, Table1. The entrance angles of abutment at the upstream are changed five times (90°, 60°, 45°, 30°, 15°, and 10°), (Photo 2). The total number of experiments is 90. Details of the experimental conditions are summarized in Table 1. Fig. 2, presents the required time for each test, in which the relationship between $d_s/d_{s\ \mathrm{Equilibrium}}$ was plotted against the time. It was found that 90% of maximum scour depth was achieved at 2 h.

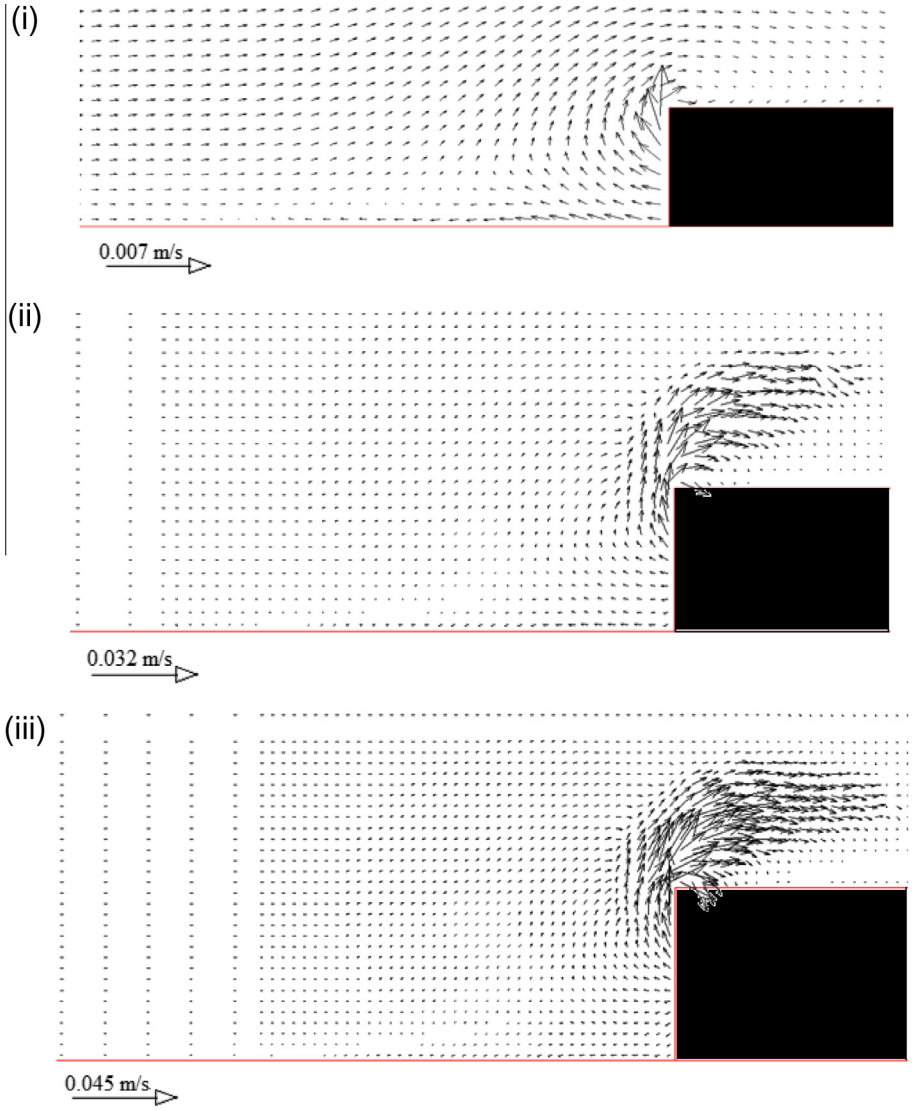

Figure 6 Horizontal velocity distribution over mobile bed by distance 0.1% of water depth, for (i) $e = 0.17$, (ii) $e = 0.25$, and (iii) $e = 0.37$ at $F_t = 0.35$.

Please cite this article in press as: Mohamed, Y.A. et al., Experimental and theoretical investigations of scour at bridge abutment. Journal of King Saud University – Engineering Sciences (2013), http://dx.doi.org/10.1016/j.jksues.2013.09.005

3. The numerical model

The SSIIM program solves the Navier–Stokes equations with the k-ε on a three dimensional and general non-orthogonal co-ordinate. These equations are discretized with a control volume approach. An implicit solver is used, producing the velocity field in geometry. The velocities are used when solving the convection–diffusion equations. The Navier–Stokes equations for non-compressible and constant density flow can be modeled as:

$$\frac{\partial u_i}{\partial t} + U_j \frac{\partial u_i}{\partial x_j} = \frac{1}{\rho} \frac{\partial}{\partial x_j} \left[-p\partial_{ij} - \rho \overline{u_i u_j} \right] \quad (1)$$

The left term on the left side of theEq. (1) indicates the time variations. The next term is the convective term. The first term on the right-hand side is the pressure term and the second term on the right side of the equation is the Reynolds stress. The Reynolds stress is evaluated using the turbulence model k–ε. The free surface is calculated using a fixed-lid approach, with zero gradients for all variables. The locations of the fixed lid and its movement as a function of time and water flow field are computed by different algorithms. The 1D backwater computation is the default algorithm and it is invoked automatically. Formula developed by Van Rijn, 1987 was used to calculate the equilibrium sediment concentration close to the bed. This equation has the form:

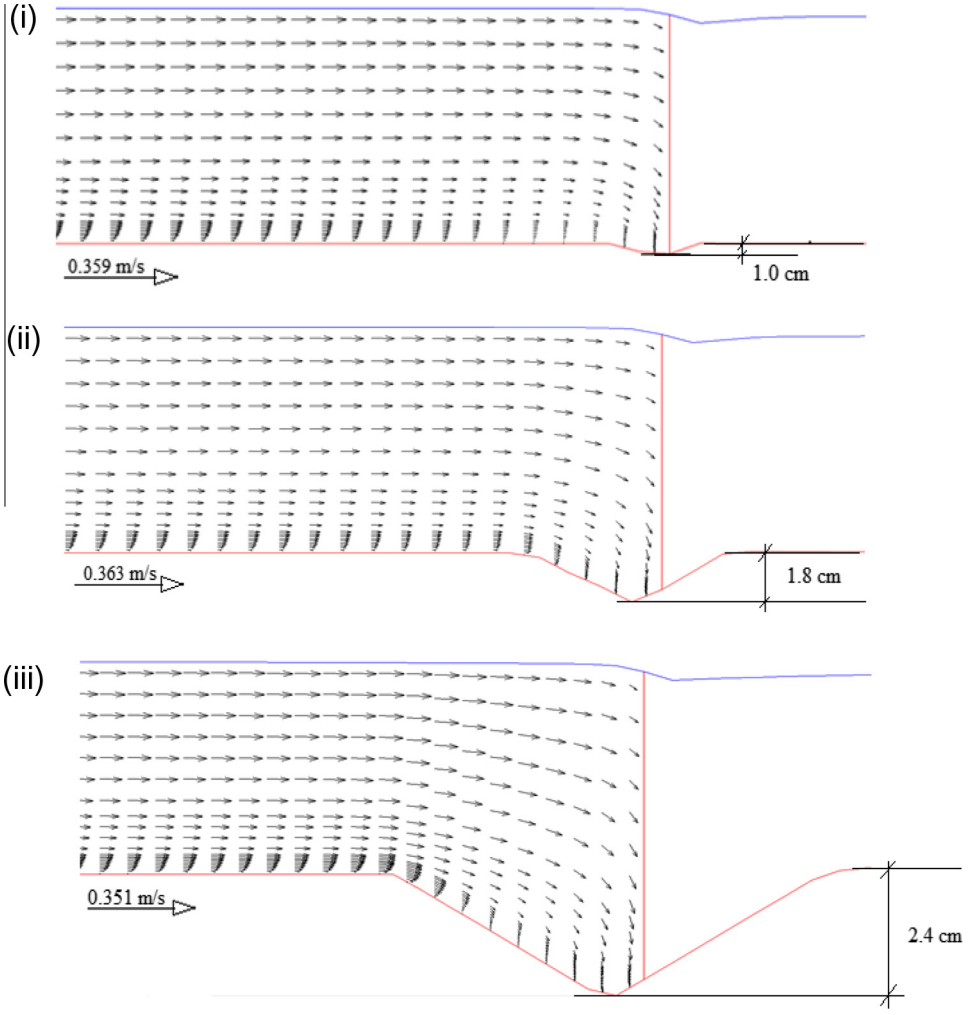

Figure 7 Velocity distribution for elevation cross-section at the end of bridge abutment, for (i) $e = 0.17$, (ii) $e = 0.25$, and (iii) $e = 0.37$ at $F_t = 0.35$.

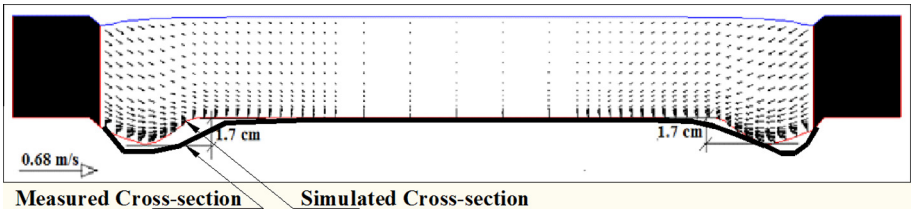

Figure 8 Measured and simulated cross-section for contraction ratio equals 0.17 at $F_t = 0.42$.

$$C_{bed} = 0.015\frac{d^{0.3}[(\tau-\tau_c)/\tau_c]^{1.5}}{a[((\rho_s-\rho_w)g)/(\rho_w v^2)]^{0.1}} \quad (2)$$

where C_{bed} is the sediment concentration, d is the sediment particle diameter, a is a reference level set equal to the roughness height, τ is the bed shear stress, τ_c is the critical bed shear stress for the movement of sediment particles according to Shield's curve, ρ_w and ρ_s are the density of water and sediment, respectively, v is the Kinematic viscosity of the water and g is the gravitational acceleration.Van Rijen's formula, 1987 is used to calculate the bed load discharge (q_b), the equation has the following form:

$$\frac{q_b}{D_{50^{1.5}}\sqrt{((\rho_s-\rho_w)g)/\rho_w}} = 0.053\frac{d^{0.3}[(\tau-\tau_c)/\tau_c]^{1.5}}{D_{50}^{0.3}[((\rho_s-\rho_w)g)/(\rho_w v^2)]^{0.1}} \quad (3)$$

where D_{50} is the mean size of the sediment.

The influence of rough boundaries on fluid dynamics is modeled through the inclusion of the wall law:

$$\frac{U}{U_*} = \frac{1}{K}\ln(30z/K_s) \quad (4)$$

where k_s is equal to the roughness height, K is von Karmen constant, U is the mean velocity, U_* is the shear velocity and z is the height above the bed.

4. Model geometry and properties

A structured grid mesh on the x–y–z plane was generated. A three dimensional grid mesh with 234 elements in the x-direction, 66 elements in the y-direction and 22 elements in the z-direction was obtained. An uneven distribution of grid lines in both horizontal and vertical directions was chosen in order to keep the total number of cells in an acceptable range and to get valuable results in the area. The following grid line distributions were chosen: In X-direction: 3 cells with a 0.25 m, 10 cells with a 0.05 m, 25 cells with a 0.02 m, 160 cells with a 0.005 m, 20 cells with a 0.02 m, 10 cells with a 0.05 m and 5 cells with a 0.11 m, respectively. In Y-direction: 30 cells with a 0.005 m, 5 cells with a 0.02 m and 30 cells with a 0.005 m, respectively. In Z-direction: 10 cells with 1% height of the water depth, 4 cells with 5% of the water depth and 7 cells with 10% of the water depth. The abutment was generated by specifying its ordinates, and then the grid interpolated using the elliptic grid generation method. However, the abutment was generated by blocking the area of the abutment.

5. Analysis and discussion

5.1. The effect of contraction ratio of bridge $e = 2b/B$ on local scour depth

In this section, the effect of different widths of abutment on local scour depth was investigated experimentally and theoretically for the 90° entrance angle of abutment. The width of bridge abutment was changed to have three contraction ratios ($e = 2b/B = 0.37$, 0.25, and 0.17), where, B is the channel width and b is the abutment width. The relationship between the tail Froude number F_t and the relative scour depth at bridge abutment d_s/y_t, (y_t, is the tail water depth) is shown in Fig. 3, for the different contraction ratios (e). This figure shows that, as the contraction ratio (e) increases the local scour depth increases and vice versa. In addition, the relative scour depth increases as the tail Froude number increases. The scour contour maps for contraction ratios (e) = 0.17, 0.25, and 0.37 are presented in Fig. 4. It is clearly shown that the scour hole dimension for contraction ratio (e) = 0.17 is smaller compared to the other contraction ratios (e) = 0.25 and 0.37. The velocities created around bridge abutment increase as the contraction ratios increase and then larger scour depth will be created. The results of Garde et al. (1961) are plotted in Fig. 3 for contraction ratio and median grain size of sediment equal to 0.37 and 2 mm, respectively. The theoretical values of local scour depth created by the 3-D computational fluid dynamic model are compared to the measured data, see Fig. 5. The correlation coefficient between the simulated and the experimental values is 95% and the mean relative absolute error is 12%. So, it is obvious that the 3D simulation model expresses well the scour phenomenon at bridge abutment. The velocity distributions around the bridge abutment in both of horizontal and vertical direction are presented in Figs. 6 and 7, respectively. It was clearly found that, as the contraction ratio increases the velocity concentration increases at the edge of bridge abutment in both horizontal and vertical directions. The downward velocity is larger for (e) = 0.37 compared to the others (e) = 0.25 and 0.17. The velocity concentration with large values at the abutment is the main reason for formation of large values of local scour depth. Measured and simulated cross-section for contraction ratio equals 0.17 at F_t = 0.42 is presented in Fig. 8. It was found that the simulated results matched with experimental data, ensuring the capabilities of the 3-D computational fluid dynamic model to simulate the scour at the bridge abutments.

5.2. Effect of entrance angles (θ) of bridge abutment on local scour depth

For the contraction ratio, e = 0.37, the relationship between the relative scour (d_s/y_t) depth and Froude number F_t for

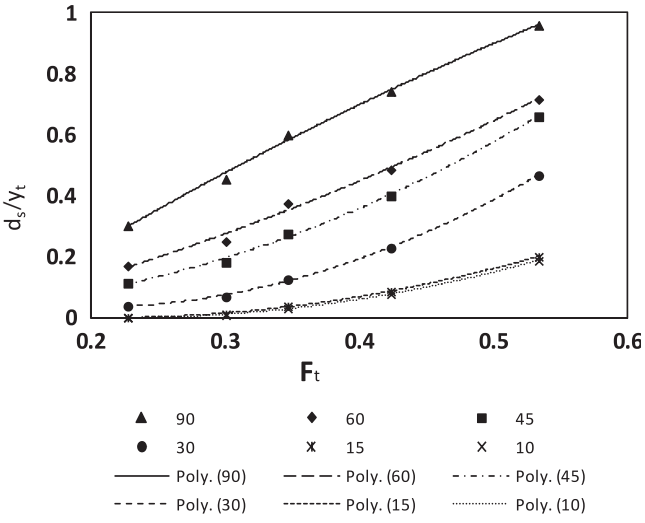

Figure 9 The relationship between the relative scour depth (d_s/y_t) and Froude number F_t for different entrance angles of bridge abutments.

different entrance angles upstream the abutment is shown in Fig. 9. It was found that the sharp entrance angle ($\theta = 90°$) at the upstream of the abutment produces higher values of scour depth compared to the other angles. In addition, the milder slopes of entrance angles produce smaller values of local scour depth, i.e. 10°, and 15°. The local scour depth was reduced in average by 37%, 50%, 74%, 91%, and 92% for the abutment face angles 60°, 45°, 30°, 15°, and 10°, respectively

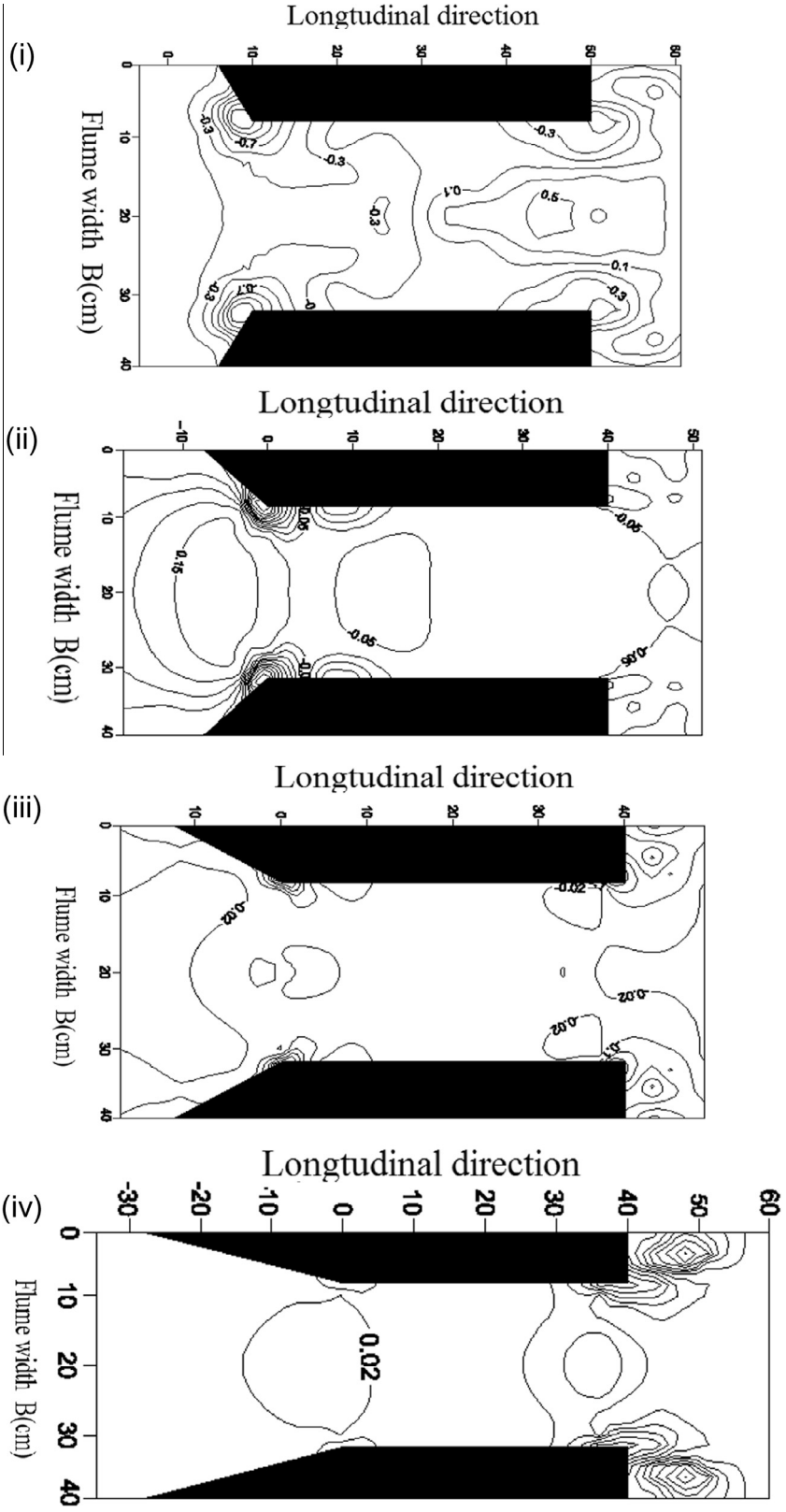

Figure 10 Scour contour maps for (i) $\theta = 60°$, (ii) $\theta = 45°$, (iii) $\theta = 30°$, and (iv) $\theta = 15°$ at $F_t = 0.35$.

compared to $\theta = 90°$. The same results can be investigated through the scour contour maps for typical cases in Fig. 10. This figure shows that, the scour around the abutment with face slope equal to 15° and 10° is smaller than the other angles of bridge abutment, (i.e. Fig. 4iii, and Fig. 10i–iii). The results of the 3D-Computational fluid dynamic model are presented in Fig. 10 at which the experimental values of local scour depth compared to the simulated ones, for different entrance angles of the bridge abutment. It was found that the selected models produce scour depths close to the experimental values with correlation coefficient $R^2 = 99\%$ and mean relative absolute error of 10%. In general, forming of scour at the abutment edge can be clearly explained using the velocity distribution as shown in Fig. 12 for a typical case of entrance angle 15°. This figure shows the velocity distribution in both horizontal and vertical directions. This figure explains the smaller values of scour at the bridge abutment. Small values of downward velocity, (Fig. 12ii) and good distribution of horizontal velocity, (Fig. 12i) are generated. From the above analysis it is highly recommended to overcome and reduce the actions of such velocities formed at bridge abutments by using anti-scour devices (see Fig. 11).

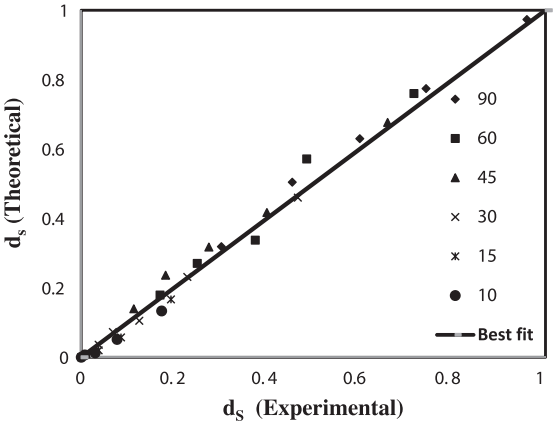

Figure 11 Simulated versus experimental for (d_s/y_t) for different entrance angles.

6. Conclusions

The present study focuses on experimental and numerical simulation of maximum depth of scour around bridge abutment in sandy soil. Different expansion ratios of channel width and entrance angles of bridge abutment are examined experimentally and by employing a 3D numerical model (SSIIM program). It was found that the local scour depth at bridge abutment increases as the contraction ratio increases. In addition, the milder entrance angles ($\theta = 10°$ and 15°) of bridge abutment produce smaller values of local scour depth compared to the steeper ones. The local scour depth at bridge abutment is reduced by 92% by applying entrance angle of 10° compared to the entrance angle of 90°. In addition, the simulated results show the ability of SSIIM for modeling the local scouring at bridge abutments having different contraction ratios of channel width and entrance angles with an average correlation coefficient of 97%.

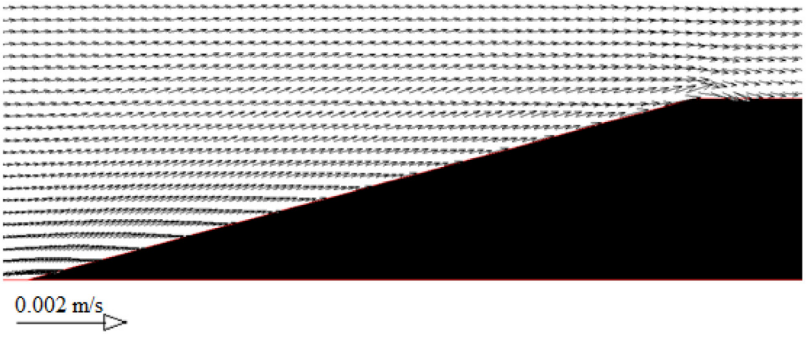

(i) Plan cross-section (at distance 0.1% of water depth)

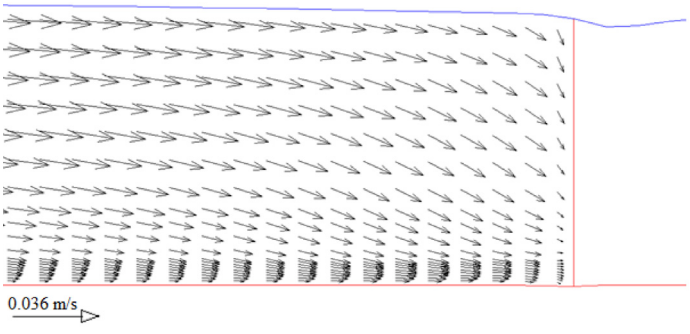

(ii) Elevation cross-section (at the end of bridge abutment)

Figure 12 Plan and elevation velocity distribution for $\theta = 15°$ at $F_t = 0.35$.

Please cite this article in press as: Mohamed, Y.A. et al., Experimental and theoretical investigations of scour at bridge abutment. Journal of King Saud University – Engineering Sciences (2013), http://dx.doi.org/10.1016/j.jksues.2013.09.005

References

Abdel-Aal, G.M., Mohamed, Y.A., 2010. The effect of collar size and shape on scour depth around bridge piers. Scientific Bulletin, Faculty of Engineering, Ain Shames University, Faculty of Engineering, Cairo, Egypt.

Abdel-Aal, G.M., Mohamed, Y.A., Waheed, E.O., El-fooly, M.M., 2008. Local scour mitigation around bridge piles using protective plate (collar), Scientific Bulletin, Faculty of Engineering, Ain Shames University, Faculty of Engineering, Cairo, Egypt, Vol. 2, September, pp. 343–354.

Abou-Seida, Mostafa, T.M.S., lsaeed, G.H., Elzahry, E.F.M., 2009. Experimental investigation of abutment scour in sandy soil. J. Appl. Sci. Res. 5 (1), 57–65, Faculty of Engineering (Shoubra), Benha University, Egypt.

Alabi P.D., 2006. Time development of local scour at bridge pier fitted with a collar. Master degree thesis, University of Saskatchewan, Saskatoon, Saskatchewan, Canada.

Cheremisinoff, P.N., Cheremisinoff, N.P., Cheng, S.L., 1987. Hydraulic Mechanics 2. Civil Engineering Practice. Technomic Publishing Company Inc., Lancaster, Pennsylvania, U.S.A..

Chiew, Y.M., 1992. Scour protection at bridge piers. J. Hydraul. Eng., ASCE, 1260–1269.

Dehghani A.A., Esmaeili T., Kharaghani S., Pirestani M.R., 2009. Numerical simulation of scour depth evolution around bridge piers under unsteady flow condition. Water Engineering for a Sustainable Environment. Vancouver: IAHR, pp. 5888–5895.

Dou, X. 1997. Numerical simulation of three-dimensional flow field and local scour at bridge crossings. Ph.D. Dissertation. University of Mississippi, Oxford, MS, U.S.A.

Fathi, A., Zarrati, A., Salamatian, A., 2011. Scour depth at bridge abutments protected with a guide wall. Can. J. Civ. Eng. 38 (12), 1347–1354.

Garde, R.J., Subramanya, K., Nambudripad, K.D., 1961. Study of scour around spur-dikes. J. Hydraul. Div. Proc. Am. Soc. Civ. Eng. 87 (6), 23–37.

Gaudio, R., Tafarojnoruz, A., Calomino, F., 2012. Combined flow-altering countermeasures against bridge pier scour. J. Hydraul. Res. 50 (1), 35–43.

Grimaldi, C., Gaudio, R., Calomino, F., Cardoso, A.H., 2009. Countermeasures against local scouring at bridge piers: slot and combined system of slot and bed sill. J. Hydraul. Eng., ASCE, 425–432.

Hua Li, 2005. Countermeasures against scour at bridge abutments. PhD Thesis, Michigan Technological University.

Kose, O., Yanmaz, M.A., 2010. Scouring reliability of bridge abutments. Aksaray University, Aksaray, Turkey. Middle East Technical University, Ankara, Turkey. Teknik Dergi 21 (1), 4919–4934.

Melville, B.W., 1992. Local scour at bridge abutment. Journal of Hydraulic Engineering 118 (4), 615–631.

Melville, B.W., 1997. Pier and abutment scour: integrated approach. Hydraul. Eng., ASCE 123 (2), 125–136.

Mohammadpour, R., Ghanib, A., Azamathullac, H.M., 2013. Estimation of dimension and time variation of local scour at short abutment. Int. J. River Basin Manage..

Moncada-M, A.T., Aguirre-Peb, J.C., Bolívarc, Floresd, E.J., 2009. Scour protection of circular bridge piers with collars and slots. J. Hydraul. Res. 47 (1), 119–126.

Morales, R., Ettema, R., 2011. Insights from depth-averaged numerical simulation of flow at bridge abutments in compound channels. Department of Civil and Architectural Engineering University of Wyoming Laramie, WY 82071, vol. 701, pp. 231–7708.

Mowafy, M.H., EI-Sayed, A.H., 2000. Effect of weeds accumulation on scour depth around bridge piers. Eng. Res. J., Helwan Univ. 70, 83–94, Faculty of Engineering, Cairo, Egypt.

Mowafy, M.H., Fahmy, M.R., 2001. The effect of constructing two adjacent bridges on the flow characteristics and local scour around bridge piers. Sci. Bull. Faculty Eng. 36 (1), 129–141. Ain shams university, Cairo, Egypt.

Odgaard, A.J., Wang, Y., 1987. Scour prevention at bridge piers. In: Proceeding of Hydraulic Engineering National Conference. ASCE, Ragan, Virginia, pp. 523–527.

Olsen, N.R., 2007. A three dimensional numerical model for simulation of sediment movements in water intakes with multiblock option, User's manual [Online]. Available: http://www.ntnu.no.

Olsen, N.R.B., Melaaen, M.C., 1993. Three-dimensional calculation of scour around cylinders. J. Hydraul. Eng. ASCE 119, 1048–1054.

Richardson, E.V., Abed, L., 1993. Top width of pier scour holes in free and pressure flow. Proc. Int. Conf. Hydraul. Eng. Part 1 1, 25–30.

Richardson, E.V., Davis, S.R., 2001. Evaluating Scour at Bridges, fourth ed. Federal Highway Administration Hydraulic Engineering Circular No. 18, FHWA NHI 01–001.

Richardson, J.E., Panchang, V.G., 1998. Three-dimensional simulation of scour-inducing flow at bridge piers. J. Hydraul. Eng, ASCE 124, 530–540.

Tafarojnoruz, A., Gaudio, R., Dey, S., 2010. Flow altering countermeasures against scour at bridge piers: a review. J. Hydraul. Res., 441–452.

Taymaz, E., Amir, A.D., Mohammad, R.P., Tetsuya, S., 2011. Numerical simulation of skewed slot effect on local scour reduction. Journal of Water Sciences Research 3 (1), 69–80.

Tafarojnoruz, A., Gaudio, R., Calomino, F., 2012. Bridge pier scour mitigation under steady and unsteady flow conditions. Acta Geophys. 60 (4), 1076–1097.

Tseng, M.H., Yen, C.L., Song, C.S., 2000. Computation of three dimensional flow around square and circular piers. Int. J. Numer. Meth. Fluids 122, 120–128.

Van Rijn, L. C., 1987. Mathematical modeling of morphological processes in the case of suspended sediment transport. Ph.D. Thesis, Delft University.

Zarrati, A.M., Gholami, H., Mashahir, M.B., 2004. Application of collar to control scouring around rectangular bridge piers. J. Hydraul. Res., IAHR 42 (1), 97–103.

Zarrati, A.M., Nazariha, M., Mashahir, M.B., 2006. Reduction of local scour In the vicinity of bridge pier groups using collars and riprap. J. Hydraul. Eng., ASCE 132 (2), 154–162.

Please cite this article in press as: Mohamed, Y.A. et al., Experimental and theoretical investigations of scour at bridge abutment. Journal of King Saud University – Engineering Sciences (2013), http://dx.doi.org/10.1016/j.jksues.2013.09.005